DRAFT

Proceedings of the 14th International Heat Transfer Conference
IHTC14
August 8-13, 2010, Washington D.C., USA

IHTC14-23176

MEASUREMENT OF LIQUID FILM THICKNESS IN MICRO TUBE ANNULAR FLOW

Hiroshi Kanno
The University of Tokyo
Hongo, Tokyo, Japan

Youngbae Han
The University of Tokyo
Hongo, Tokyo, Japan

Yusuke Saito
The University of Tokyo
Hongo, Tokyo, Japan

Naoki Shikazono
The University of Tokyo
Hongo, Tokyo, Japan

ABSTRACT

Heat transfer in micro scale two-phase flow attracts large attention since it can achieve large heat transfer area per density. At high quality, annular flow becomes one of the major flow regimes in micro two-phase flow. Heat is transferred by evaporation or condensation of the liquid film, which are the dominant mechanisms of micro scale heat transfer. Therefore, liquid film thickness is one of the most important parameters in modeling the phenomena. In macro tubes, large numbers of researches have been conducted to investigate the liquid film thickness. However, in micro tubes, quantitative information for the annular liquid film thickness is still limited. In the present study, annular liquid film thickness is measured using a confocal method, which is used in the previous study [1, 2]. Glass tubes with inner diameters of 0.3, 0.5 and 1.0 mm are used. Degassed water and FC40 are used as working fluids, and the total mass flux is varied from G = 100 to 500 kg/m^{2}s. Liquid film thickness is measured by laser confocal displacement meter (LCDM), and the liquid-gas interface profile is observed by a high-speed camera. Mean liquid film thickness is then plotted against quality for different flow rates and tube diameters. Mean thickness data is compared with the smooth annular film model of Revellin et al. [3]. Annular film model predictions overestimated the experimental values especially at low quality. It is considered that this overestimation is attributed to the disturbances caused by the interface ripples.

1. INTRODUCTION

Heat transfer in micro tube attracts large attention since it has many advantages, e.g., high efficiency, miniaturization, and stability of flow regimes. In micro tubes, flow characteristics are quite different from those in macro tubes, since surface tension becomes dominant in micro scale. At high quality, annular flow is one of the major flow patterns, and film evaporation or condensation dominates heat-transfer in micro tubes. Therefore, thin liquid film thickness plays an important role in micro scale heat transfer, and many studies concerned with film thickness and interface profiles in annular flow regimes have been conducted.

Schubring and Shedd [4] investigated film thickness in horizontal annular air-water flow using the diffused light pattern reflected from the liquid surface. Working fluids were air and water. Glass tubes with inner diameters of 8.8 mm and 15.1 mm were used as test tubes. It was reported that wave velocity of annular film was well correlated by the gas friction velocity. This indicated a direct link between wave velocity and wall shear stress.

Hazuku et al. [5] measured liquid film thickness in glass tube with inner diameter of 11 mm using laser confocal displacement meter. The data from this method agreed with that from image processing method. They concluded that the liquid film thickness decreases due to the density change of the gas phase.

Okawa et al. [6] also investigated film behavior in annular two-phase flow using laser confocal method. They introduced steam-water two-phase flow in heated SUS tube with inner diameter of 12 mm. They controlled total mass flux and heat flux to produce flow oscillation. They concluded that mean film thickness in the thin film region tends to increase with the decrease of oscillation period.

Revellin et al. [7] measured flow pattern characteristics in micro tubes with inner diameter of 0.5 mm. Working fluid was R-134a and they applied direct current to heat the SUS tube. They measured bubble frequency and superficial vapor velocity by laser light intensity method. In their research, flow patterns and their transitions (bubbly/slug flow/semi-annular flow) were detected by bubble frequency analysis.

Han and Shikazono [1] measured liquid film thickness of slug flow by the confocal method. They used glass tubes with inner diameters of 0.3, 0.5, 0.7, 1.0 and 1.3 mm as test tubes.

Working fluids were water, ethanol, and FC40. They proposed empirical correlation for the dimensionless liquid film thickness based on capillary, Reynolds and Weber numbers. They concluded that no inertial force effect is observed at small capillary numbers, while Reynolds number effect becomes apparent at large capillary numbers.

Tibrisa et al. [8] reviewed measurement methods of liquid film thickness in micro scale. They pointed out that the confocal method allowed dynamic measurements of extremely thin film, and its use should be worth considered for future studies.

Although many researches for liquid film thickness have been carried out, quantitative data of annular film in micro scale is still limited. To predict heat-transfer coefficient in micro scale two-phase flow, it is important to clarify the relationship between flow regime and liquid film thickness in micro tube annular flow. In the present study, liquid film thickness is measured and flow regime is observed in micro scale annular flow. The relationship between film thickness and flow characteristics is investigated.

NOMENCLATURE

A	cross sectional area [m^2]
C_f	Fanning friction factor
D	tube diameter [mm]
G	mass flux [kg/m^2s]
L	length [mm]
$\dot{m}$	mass flow rate [kg/s]
n	refractive index
P	pressure [kPa]
Re	Reynolds number, $Re = \rho UD/\mu$
T	temperature [$^\circ$C]
U	velocity [m/s]

Greek symbols

δ	liquid film thickness [μm]
μ	viscosity [μPa s]
ρ	density [kg/m^3]
σ	surface tension [mN/m]
τ	shear stress [mN/m]

Subscripts

air	air
l	liquid
vl	between vapor and liquid
wl	between wall and liquid

2. EXPERIMENTAL SETUP AND PROCEDURE

The experimental setup used in the present study is shown in Fig. 1. Compressed air and liquid from syringe pump are introduced to the inlet block and they are mixed at the T-junction. Then, two-phase air-liquid mixture is introduced in the test tube. Pressure was measured at the inlet and outlet blocks.

Circular glass tubes with inner diameters of 0.3, 0.5 and 1.0 mm were used. Length to diameter ratio is fixed as L/D = 300. Each edges of the glass tube were connected to the inlet and outlet blocks. The T-junction in the inlet block is shown in Fig. 2.

Figure 3 shows the test section and the measurement position. The total length L is defined as the distance from the inlet pressure port to the outlet pressure port. Liquid film thickness and flow regime are measured at the position 0.833L downstream from the inlet pressure port.

Mass flow controllers (MQV9200, MQV0005, MQV0050, Yamatake) were used to control the airflow rate, and syringe pump (IP7100, Lab-Quatec) was used to control the liquid flow rate. Liquid was drawn from the reservoir tank through 20 μm or 60 μm filters. Pressure sensors (AP-10S, AP-13S, Keyence) were used to measure the pressure gradient of the test tubes.

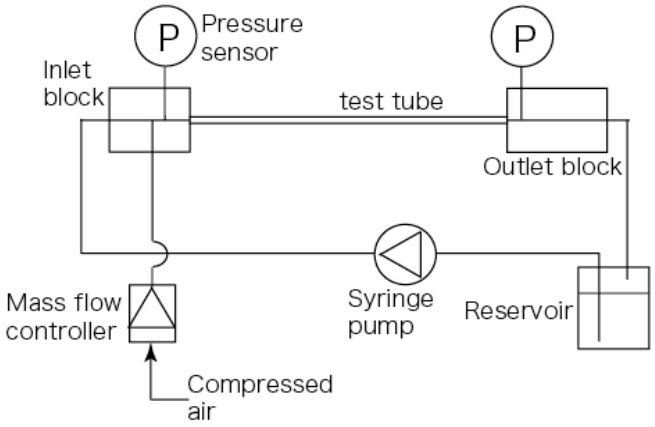

Fig. 1. Diagram of the experimental setup

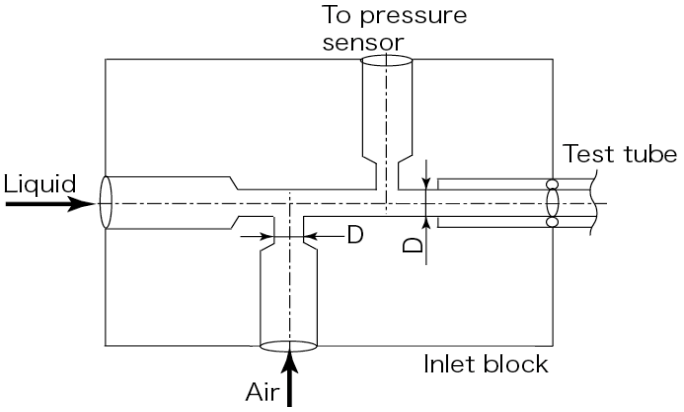

Fig. 2. T-junction of inlet block

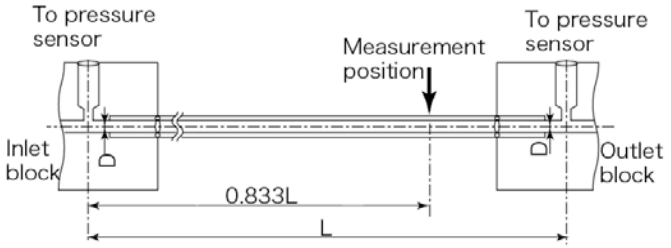

Fig. 3. Test section and measurement position

Air is used for the gas phase, and to clarify the effects of inertial and viscous forces, water and FC40 were used for the liquid phases. All experiments were conducted under the condition of room temperature. Table 2 shows the properties of the working fluids at 20 and 25˚C.

Total mass flux is controlled as G = 100, 300 and 500 kg/m^{2}s. Superficial air and liquid velocities are calculated according to Eqs. (1) and (2), where x is flow quality, ρ is density, A is total flow area and D is inner diameter.

$$U_{air} = \frac{Gx}{\rho_{air}} \tag{1}$$

Table 2 Properties of the working fluids at 20 and 25˚C

	Temperature (˚C)	Water	FC40
ρ (kg/m^3)	20	998	1860
	25	997	1849
μ (μpa s)	20	1001	3674
	25	888	3207
σ(mN/m)	20	72.7	16.3
	25	72.0	15.9
n		1.33	1.29

$$U_{liquid} = \frac{G(1-x)}{\rho_{liquid}} \tag{2}$$

$$x = \frac{\dot{m}_{air}}{\dot{m}_{air} + \dot{m}_{liquid}} \tag{3}$$

$$G = \frac{\dot{m}_{air} + \dot{m}_{liquid}}{A} \tag{4}$$

$$Re_{air} = \frac{G(1-x)D}{\mu_{air}} \tag{5}$$

$$Re_{liquid} = \frac{GxD}{\mu_{liquid}} \tag{6}$$

Laser confocal displacement meter (LT9010M, Keyence) is used to measure the liquid film thickness. This method is used in our previous studies [1, 2]. It is reported that the laser confoal displacement meter can measure the liquid film thickness very accuracy within 1% error [5]. The resolution for the present laser confocal displacement meter is 0.01 μm, and the spot diameter of the laser is 2 μm. Sampling frequency is 1 kHz, and 5,000 data points for 5 seconds are collected for each run. Dimensionless mean thickness δ/D is calculated for each diameter of test tubes and plotted against quality.

Flow regime was observed by using high-speed camera (SA1.1, Photron). Frame rate is 20,000 frames per second with a shutter time of 5.3 μs. Figure 4 shows the cross section of the measuring point. To remove the outer wall curvature effect, two slides of cover glass were put on both sides of the glass tube and glycerol is filled in between them. The refractive index of glycerol is almost same as that of Pyrex glass. Therefore, the outer-wall curvature effect can be removed and inner-liquid surface can be visualized clearly.

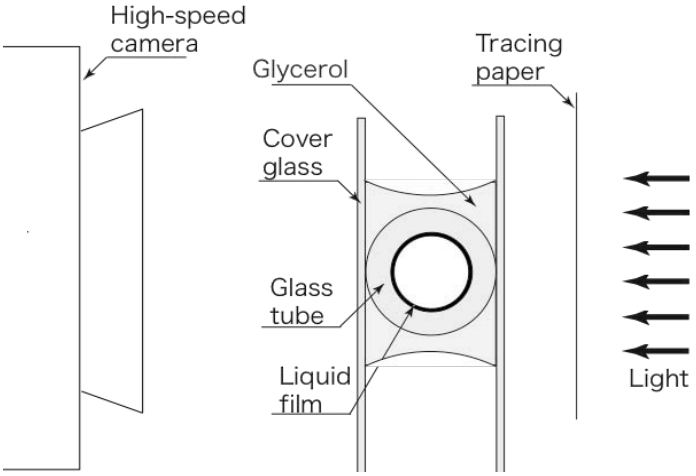

Fig. 4. Test section for high-speed camera observation

3. RESULTS AND DISCUSSION

3.1 Dimensionless mean thickness and flow regime

Figure 5 shows the flow patterns for D = 0.5 mm tube at G = 300 kg/m^{2}s. Inner-liquid surface is visualized clearly. Ripples on the interface between liquid and air are observed. As quality x increases, liquid film thickness becomes thinner and the size of ripple decreases for both water and FC40. At x = 0.94, the shape of the ripples of both fluids are nearly the same, but at low quality, ripple size of FC40 is smaller and its shape is sharper. Viscosity of FC40 is about 4 times larger, and surface tension of FC40 is about 4 times smaller than those of water. The differences of the ripple shape and size are thus due to viscosity and surface tension differences.

Figure 6 shows the flow patterns for x = 0.95 at G = 300 kg/m^{2}s. Ripples are observed in all conditions. At D = 0.3 mm, however, ripple size is smaller than those in larger diameters. It is considered that the size of ripples decreases and interface becomes smoother as liquid Reynolds number gets smaller.

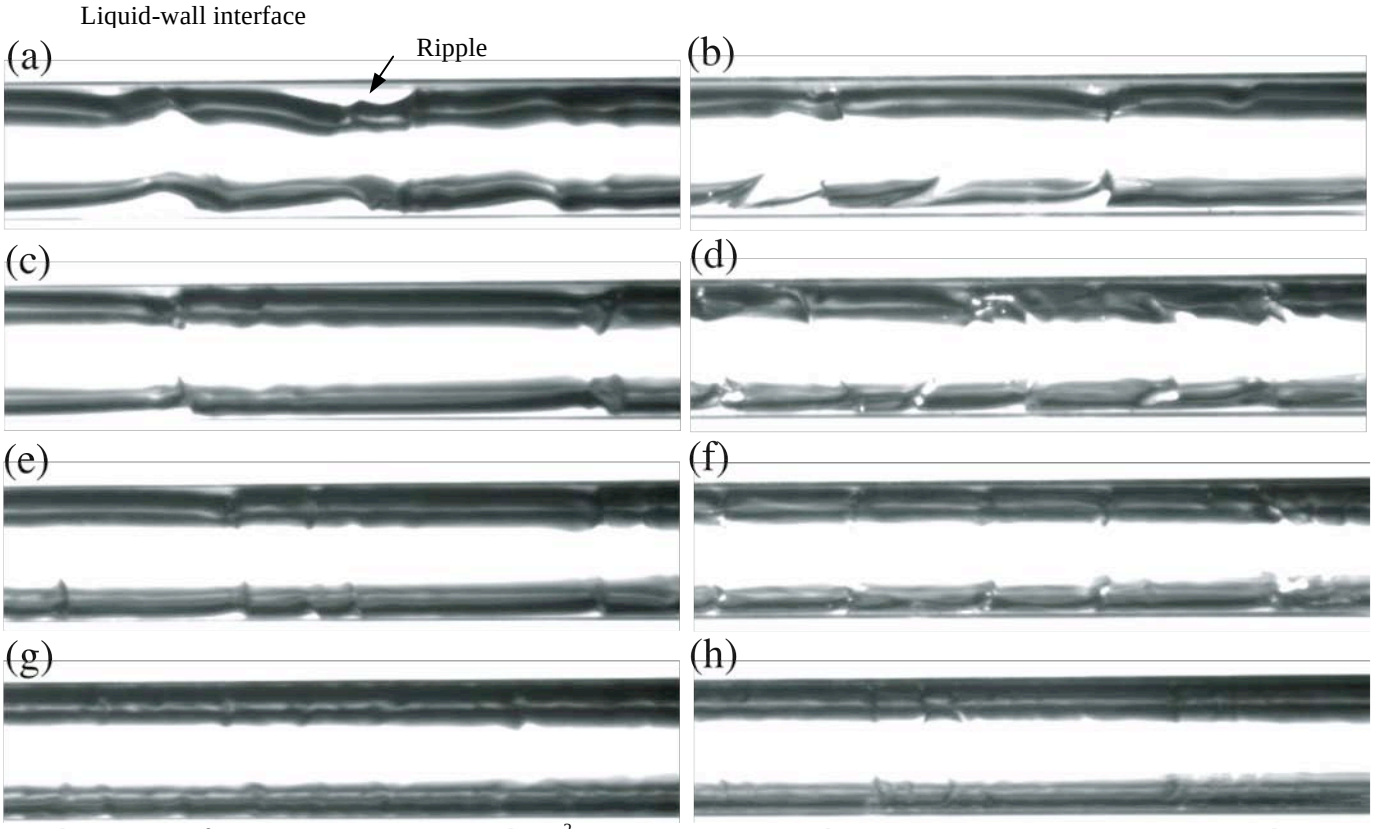

Fig. 5. Flow patterns for D = 0.5 mm, G = 300 kg/m^{2}s: (a) water, x = 0.15; (b) FC40, x = 0.15; (c) water, x = 0.44; (d) FC40, x = 0.44; (e) water, x = 0.73; (f) FC40, x = 0.73; (g) water, x = 0.94; (h) FC40, x = 0.94.

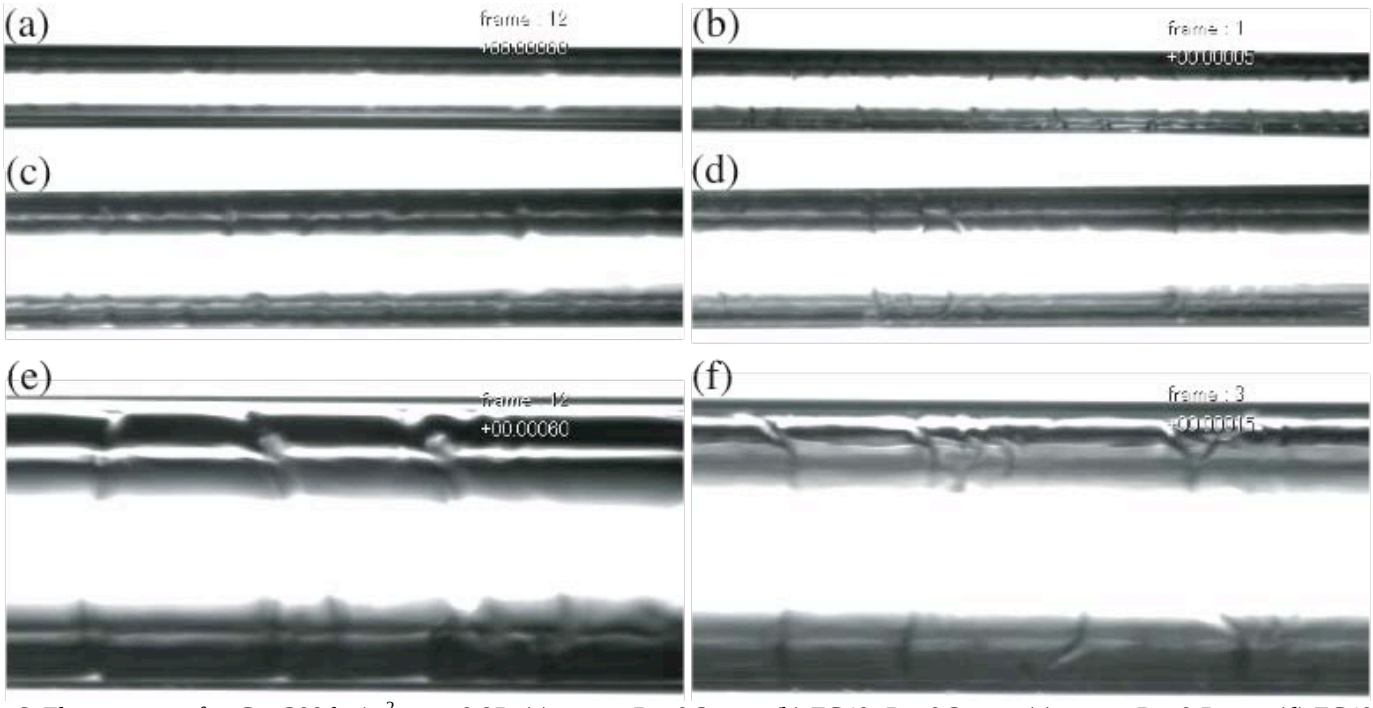

Fig. 6. Flow patterns for G = 300 kg/m^{2}s, x = 0.95: (a) water, D =0.3 mm; (b) FC40, D =0.3 mm; (c) water, D =0.5 mm; (d) FC40, D =0.5 mm; (e) water, D =1.0 mm; (f) FC40, D =1.0 mm

Figure 7 shows dimensionless mean liquid film thicknesses of water and FC40 in D = 0.5 mm tube. Mean thickness decreases with increasing x and G. In Fig. 7, mean thickness of FC40 is thicker than that of water at G = 100 kg/m^{2}s. However, mean thicknesses of FC40 become thinner at G = 300 kg/m^{2}s and 500 kg/m^{2}s. From the flow pattern observation, frequency and size of ripples become larger as mass flux increases. In addition, the numbers of ripples observed are larger for FC40 at high mass flux. In annular flow, liquid-phase is trailed by the gas-phase. Ripple increases the interfacial shear stress, which increases the liquid-phase velocity. It is considered that this interface instability makes liquid film thinner.

Figure 8 shows the dimensionless thicknesses of water and FC40 for different diameters at G = 300 kg/m^{2}s. In Fig. 8, mean thickness of FC40 is thicker than that of water at D = 0.3 mm. However, thicknesses for both fluids are nearly the same at D = 0.5 mm and 1.0 mm. From the flow pattern observation, the size of ripples increases with D. It is considered that this increase of the ripple size reduced the liquid film thickness.

Figure 9 shows the pressure loss for D = 0.5 mm tube. Pressure loss of FC40 is higher than that of water. From x = 0 to x = 0.8, pressure loss increases according to the increase in gas velocity. From x = 0.8 to x = 1.0, pressure loss decreases gradually due to the decrease in interface instability. It can be seen from the figure that the decrease in pressure loss at high quality (x>0.8) is more prominent for FC40 than water especially at large G. This implies that interface instability of FC40 is larger than that of water at large mass flux.

Figure 10 shows the pressure loss of water and FC40 for different diameters at G = 300 kg/m^{2}s. Pressure loss becomes larger as D decreases. Again, interface seems to be unstable for FC40 than for water.

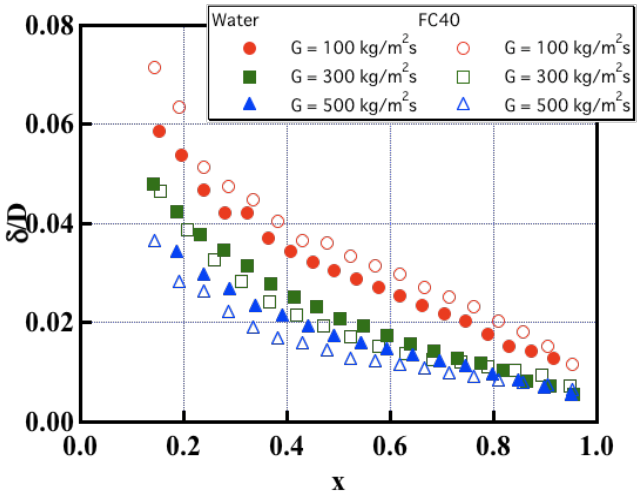

Fig. 7. Dimensionless mean thickness: D = 0.5 mm

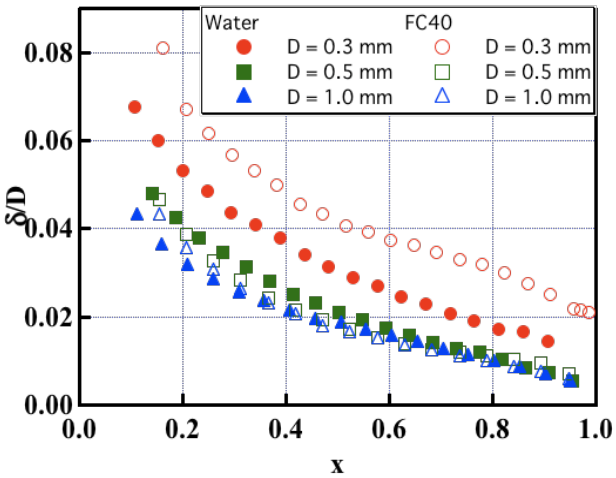

Fig. 8. Dimensionless mean thickness: G = 300 kg/m^{2}s

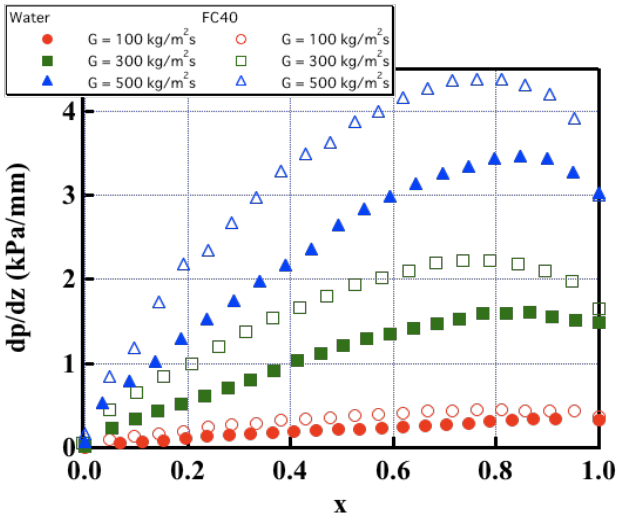

Fig.9. Pressure loss: D = 0.5 mm

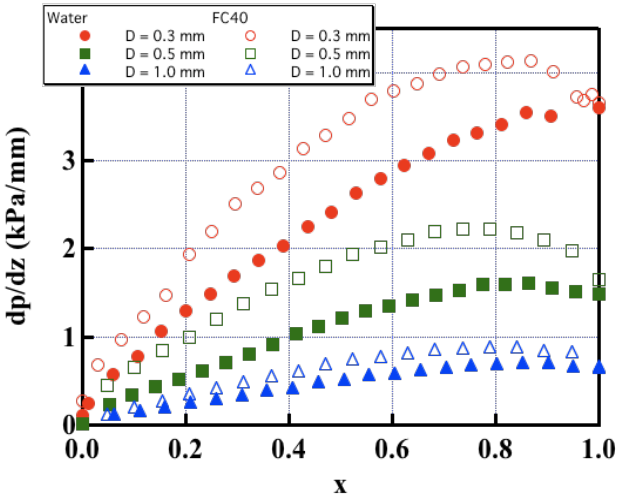

Fig. 10. Pressure loss: G = 300 kg/m^{2}s

3.2 Annular film model

To predict critical heat flux and dry-out vapor quality in micro channels, Revellin et al. [3] proposed a theoretical model for predicting annular liquid film thickness. By solving the continuity, momentum and energy equations, the liquid film thickness variation along the channel can be obtained.

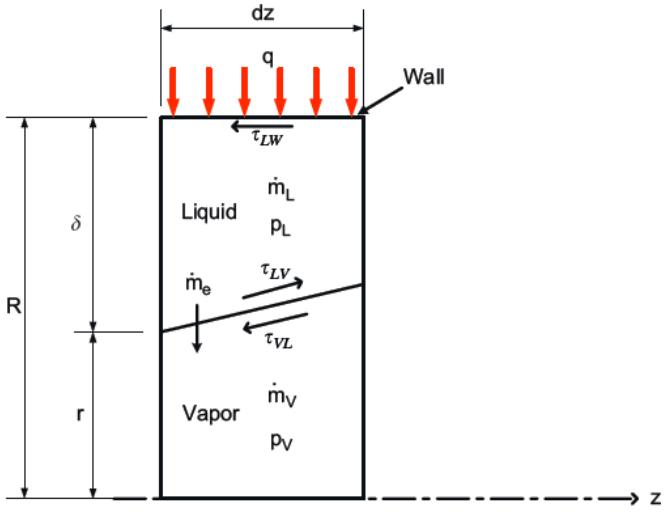

Fig. 11. Control volume of the annular film model of Revellin et al. [3]

Figure 11 shows the control volume for the Revellin et al. model. In the present study, flow condition is adiabatic, i.e. q = 0. The shear stress at the liquid and vapor interface is determined by Eqs. (7) to (9). The shear stress between wall and liquid is determined by Eqs. (10) to (12).

$$\tau_{lv} = \frac{1}{2} C_f \rho_v u_v^2 \tag{7}$$

where

$$C_f = \frac{16}{Re_v} \quad \text{For} \quad Re_v = \frac{2\rho_v u_v r}{\mu_v} < 2300 \tag{8}$$

$$C_f = 0.078 Re_v^{-0.25} \quad \text{For} \quad Re_v \geq 2300 \tag{9}$$

$$\tau_{lw} = \frac{1}{2} C_f \rho_l u_l^2 \tag{10}$$

where

$$C_f = \frac{16}{Re_\delta} \quad \text{For} \quad Re_\delta = \frac{2\rho_l u_l (R-r)}{\mu_l} < 2300 \tag{11}$$

$$C_f = 0.078 Re_\delta^{-0.25} \quad \text{For} \quad Re_\delta \geq 2300 \tag{12}$$

From the force balance, interface shear stress and wall shear stress are related as Eqs. (13) and (14). Assuming that pressure gradients of liquid and vapor phases are the same, i.e. Eq. (15), liquid film thickness can be calculated. This model assumes smooth gas-liquid interface and ignores the effects of ripples and surface tension. Thus, the effect of ripples and surface tension on the liquid film thickness can be investigated by comparing this model and our experimental results,.

$$-A_l \frac{dp_l}{dz} dz + A_i \tau_{lv} - A_{lw} \tau_{lw} = 0 \tag{13}$$

$$-A_v \frac{dp_v}{dz} dz - A_i \tau_{vl} = 0 \tag{14}$$

$$\frac{dp_v}{dz} - \frac{dp_l}{dz} = 0 \tag{15}$$

Figure 12 shows the comparison between annular film model and the present experimental data. The kinks in the prediction lines are due to laminar-turbulent transition of the gas phase. Experimental results are thinner than the model prediction, especially at low quality. At high quality, model prediction becomes closer to the experimental results. The size of ripples is very small at high quality, so it is considered that this Revelin et al. model which assumes smooth interface can predict the liquid film thickness at high qualities. However, the sizes of ripples are large especially at low quality in large diameter tubes, as shown in Figs. 5 and 6. It is considered that the difference between model prediction and experimental results can be attributed to the interface instabilities caused by the ripples, and this instability decreases the liquid film thickness. The effects of interface instabilities will be further investigated in the future work.

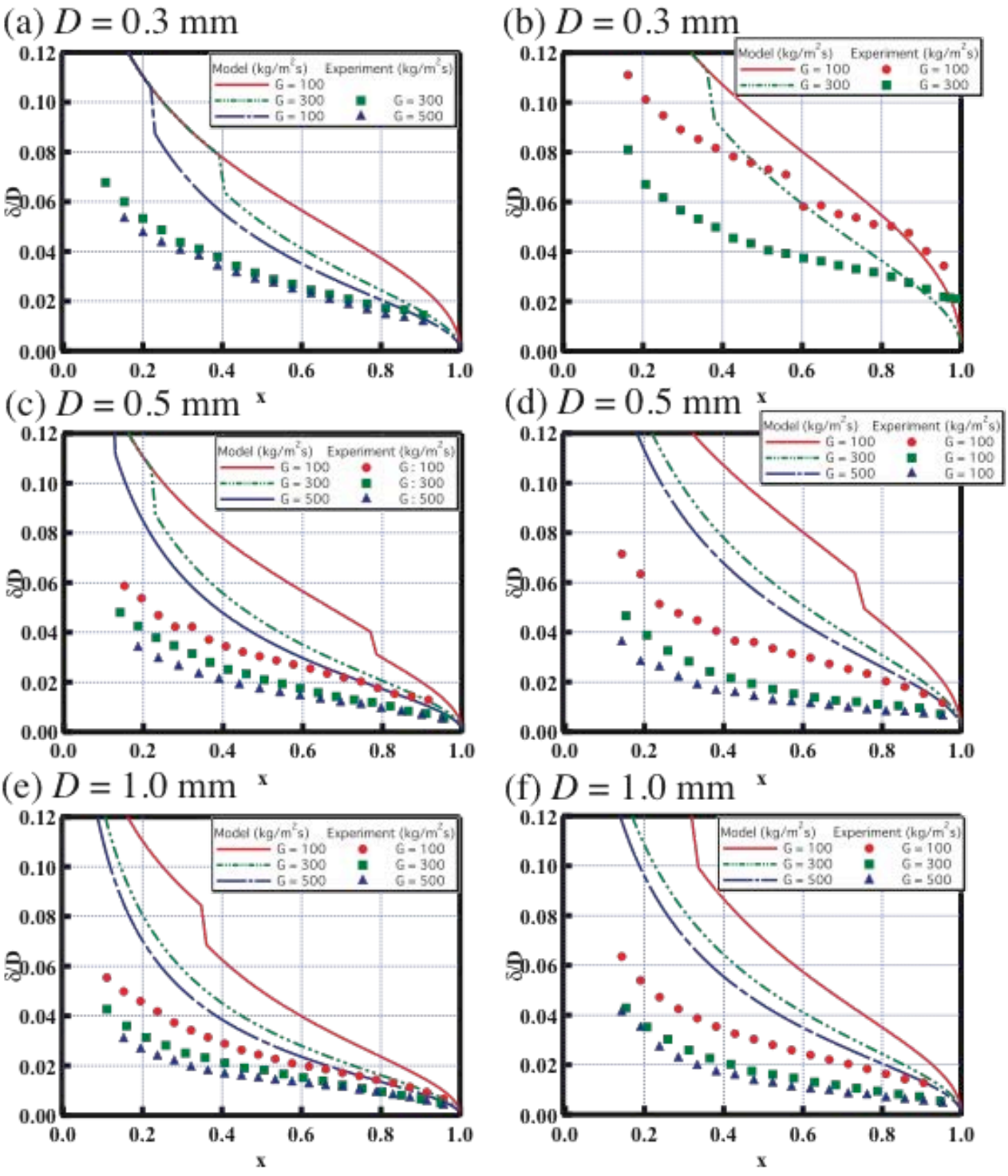

Fig. 12. Comparison between model prediction and experimental results: (a) water, D = 0.3 mm; (b) FC40, D = 0.3 mm; (c) water, D = 0.5 mm; (d) FC40, D = 0.5 mm; (e) water, D = 1.0 mm; (f) FC40, D = 1.0 mm

4. CONCLUDING REMARKS

Liquid film thickness in micro tube annular flow is measured by laser confocal displacement meter. Dimensionless mean film thickness decreases with the increase of mass flux and tube diameter. Ripples are observed from the flow pattern visualization. Inertial and surface tension forces affect the size and frequency of the ripples.

Prediction by annular film model proposed by Revellin et al. is compared with the experimental results. Experimental results are thinner than the model prediction, which is considered to be due to the interface instabilities.

ACKNOWLEDGMENTS

We would like to thank Prof. Kasagi, Prof Suzuki and Dr. Hasegawa for the fruitful discussions and advices. This work is supported through Grant in Aid for Scientific Research (No. 20560179) by MEXT, Japan.

REFERENCES

[1] Y. Han and N. Shiakzono, Measurement of the liquid film thickness in micro tube slug flow, *Int. J. Heat Fluid Flow*, 30, 842-853 (2009).

[2] Y. Han and N. Shiakzono, Measurement of the liquid film thickness in micro square channel, *Int. J. Multiphase Flow*, 35, 896-903 (2009).

[3] R. Revellin, P. Haberschill, J. Bonjour and J. Thome, Conditions of liquid film dryout during saturated flow boiling in microchannels, *Chem. Eng. Sci.*, 63, 5795-5801 (2008).

[4] D. Schubring and T. A. Shedd, Wave behavior in horizontal annular air-water flow, *Int. J. Multiphase Flow*, 34, 636-646 (2008).

[5] T. Hazuku, T. Takamasa and Y. Matusmoto, Measurement of liquid film in microchanels using a laser focus displacement meter, *Exp. in Fluids*, 38 (6), 780-788 (2005).

[6] T. Okawa, T. Goto and Y. Yamagoe, Liquid film behavior in annular two-phase flow under flow oscillation condition, *Int. J. Heat Mass Transf.*, 53, 962-971 (2010).

[7] R. Revellin, V. Dupont, T. Ursenbacher, J. Thome and I. Zun, Conditions of diabatic two-phase flows in microchannels: Flow parameter results for R-134a in a 0.5 mm channel, *Int. J. Multiphase Flow*, 32, 755-774 (2006).

[8] C. B. Tibriça, F. J. do Nascimento and G. Ribatski, Film thickness measurement techniques applied to micro-scale two-phase flow systems, *Exp. Thermal Fluid Sci.*,(2009), in press.

[9] D. Schubring and T. A. Shedd, Prediction of wall shear for horizontal annular air-water flow, *Int. J. Heat Mass Transf.*, 52, 200-209 (2009).

[10] D. Schubring and T. A. Shedd, Two-phase wavy-annular flow in small tubes, *Int. J. Heat Mass Transf.* 52, 1619-1622 (2009).

[11] S. V. Alekseenko, S.P. Aktershev, A. V. Cherdantsv, S. M. Kharlamov and D. M. Markovich, Primary instabilities of liquid film flow sheared by turbulent gas stream, *Int. J. Multiphase Flow*, 35, 617-627 (2009).